Influence of pH, multivalent counter ions, and membrane fouling on phosphate retention during ceramic nanofiltration

Kramer, F. C.; Shang, R.; Rietveld, L. C.; Heijman, S.J.G.

DOI
10.1016/j.seppur.2019.115675

Publication date
2019

Document Version
Final published version

Published in
Separation and Purification Technology

Citation (APA)
Kramer, F. C., Shang, R., Rietveld, L. C., & Heijman, S. J. G. (2019). Influence of pH, multivalent counter ions, and membrane fouling on phosphate retention during ceramic nanofiltration. *Separation and Purification Technology*, *227*, Article 115675. https://doi.org/10.1016/j.seppur.2019.115675

Separation and Purification Technology 227 (2019) 115675

Contents lists available at ScienceDirect

Separation and Purification Technology

journal homepage: www.elsevier.com/locate/seppur

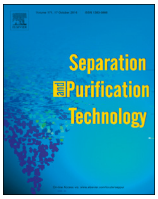

Influence of pH, multivalent counter ions, and membrane fouling on phosphate retention during ceramic nanofiltration

F.C. Kramer*, R. Shang, L.C. Rietveld, S.J.G. Heijman

Department of Sanitary Engineering, Faculty of Civil Engineering and Geosciences, Delft University of Technology, P.O. Box 5048, 2600 GA Delft, the Netherlands

ARTICLE INFO

Keywords:
Ceramic nanofiltration
Phosphate retention
Phosphate rejection
Zeta potential
Water treatment

ABSTRACT

Ceramic nanofiltration is an emerging technology for the recovery of water and nutrients (including phosphate) from municipal sewage which becomes more imperative worldwide. In order to use ceramic nanofiltration for phosphate recovery from municipal sewage, more knowledge is needed. This is the first paper reporting the phosphate retention of ceramic nanofiltration membranes. Furthermore, the influence of pH, multivalent counter ions, and membrane fouling on phosphate retention is reported in this paper. Various experiments were executed to analyse the phosphate retention and zeta potential under varying conditions. During filtration of a salt solution including phosphate, the phosphate retention increased, from 76% to 99%, with a change in pH from 5 to 9. Furthermore, magnesium ions and organic fouling had a large influence on the phosphate retention: at pH 7 the phosphate retention dropped from 92% to 42–43% due to the presence of either magnesium ions or organic fouling.

1. Introduction

The demand for water and nutrient recovery from (municipal) sewage is increasing worldwide [1–4]. An upcoming economic and sustainable alternative for the conventional sewage treatment plants are sewer mining concepts, treating municipal sewage directly for on-site usage while recovering nutrients, water, and, possibly, energy [5–7].

Ceramic nanofiltration (NF) is for several reasons an interesting technology to explore for this application. First, most components in the water can potentially be recovered, since it is based on physico-chemical separation in contrast to biological treatment. Second, membrane technology has flexibility in configuration, pore size, and membrane material which enables to tailor the treatment to achieve the highest recovery of a specific element or compound; NF has the ability to separate inorganic ions with smaller sizes and hydraulic radii than the pore size due to electrostatic repulsion in certain pH ranges [8–11]; various membrane materials have a different membrane surface charge with varying ion repulsion. Third, based on the high potential for retention of multivalent ions, this technology could support e.g. struvite production from sewage; when the concentrate stream of the NF is treated in an anaerobic digester, the digestate supernatant could afterwards be used for the production of struvite [12–15]. Fourth, ceramic membranes are susceptible to less irreversible fouling than polymeric membranes [16,17] which makes this technology more suitable for treatment of municipal sewage. Thus, theoretically, ceramic NF is an interesting technology for phosphate recovery using municipal sewage. However, the phosphate retention for those membranes have not been reported in literature yet. Nor the effect of influencing factors on the phosphate retention during ceramic NF.

In this paper ceramic NF membranes with a titanium oxide membrane layer were selected. Previous research showed that phosphate retention varies, using real municipal sewage in a bench scale sized filtration set-up with ceramic NF membranes of the same type [7]. However, no conclusive in that study was performed to determine the cause of this variation in phosphate retention. The negative charge in the pH 7–9 range [18,19] suggests that ceramic NF membranes could reject phosphate ions due to electrostatic repulsion. Moreover, Shang et al. [20] found that ceramic ultrafiltration (UF) membranes, made of similar material but with a larger pore size, had a high phosphate retention of 87% at pH 8.5 in clean water.

Literature describes that the pH and the presence of other compounds in the water can have an influence on ion retention, both in ceramic NF [18,21] and ceramic UF membranes [22]. These compounds have mainly an effect on the electrostatic interactions around the membrane surface. For instance, multivalent counter ions can cause suppression of the diffuse double layer [23–25] or can adsorb to the membrane surface which changes the surface charge of the membrane

---

* Corresponding author.
E-mail address: francakramer@gmail.com (F.C. Kramer).

https://doi.org/10.1016/j.seppur.2019.115675
Received 14 March 2019; Received in revised form 5 June 2019; Accepted 5 June 2019

Table 1
Overview of the phosphate retention and streaming potential experiments performed.

Experiment	Present during experiment				Measured	
	NaCl	H_2NaPO_4	$MgCl_2$	Fouling layer	P retention	Streaming potential
1	1 mM					X
2	1 mM			$0.8\ g{\cdot}L^{-1}$		X
3	0.7 mM	0.3 mM			X	X
4	0.7 mM	0.3 mM		$0.8\ g{\cdot}L^{-1}$	X	X
5	0.4 mM	0.3 mM	0.3 mM		X	X
6	0.4 mM	0.3 mM	0.3 mM	$0.8\ g{\cdot}L^{-1}$	X	

and thus the ion retention [26]. Thus, multivalent counter ions might also have influence on the phosphate retention during ceramic NF. In order to get insight in the electrostatic interactions on the membrane surface, streaming potential measurements are often executed to determine the membrane charge.

Another important influencing factor on the phosphate retention might be fouling on the ceramic NF membrane surface when treating municipal sewage. In literature, the influence of a fouling layer on polymeric NF membranes on ions' retention can be found [24,27–31]. Zhao et al. [17] describes a similar effect for retention of several pharmaceuticals during ceramic NF using model sewage. This suggest that a fouling layer potentially affects the phosphate retention in ceramic NF membranes when treating municipal sewage.

Both the phosphate retention in clean water and the effects of multivalent counter ions and a fouling layer on the membrane surface, especially relevant when using municipal sewage, have not been reported in literature yet. Therefore, the objective of this paper is to determine the retention (or passage) of phosphate by ceramic NF membranes in the presence of multivalent counter ions and a fouling layer on the membrane surface. This information is essential in order to be able to design a strategy for phosphate recovery from municipal sewage using ceramic NF.

2. Materials & methods

2.1. Ceramic NF membranes

Filtration experiments were performed using ceramic NF membranes with a filtration layer of titanium oxide, and with an indicated molecular weight cut-off (MWCO) of 450 Da mean pore size of 0.9 nm, and open porosity of 30–40%. The hydraulic permeability of pristine membranes was $15–20\ L{\cdot}(m^2{\cdot}h{\cdot}bar)^{-1}$ according to the supplier. The effective MWCO was measured before and after each experiment to monitor their quality, using the method described below. For the phosphate retention experiments, a single-channel, tubular configuration was used with a length of 100 mm and an effective filtration area of $0.163\ dm^2$ (Inopor GmbH, Germany).

Moreover, ceramic NF membranes with a disc configuration were used for streaming potential experiments. The disc membranes had the same specifications as the tubular membranes describe above, a diameter of 85 mm, and a specific membrane area of $0.563\ dm^2$. The disc membranes were placed in the Spirlab INSIDE DISRAM™ (TAMI) disc holder with a diameter of 90 mm.

2.2. Filtration experiments

Ceramic NF experiments were carried out with a cross-flow filtration system using a pneumatic diaphragm pump (Hydra-cell) with a pulsation dampener. The single pass water recovery of the ceramic NF system was < 1%. In addition, the feed water was recirculated; both the permeate and the concentrate were fed back into the feed tank, except for the sampling volume, which was a negligible amount (< 0.1%). The feed water composition remained constant over the duration of the experiment: this was monitored by analysing samples throughout the experiment. In order to ensure that the feed water remained constant over the duration of the experiment, feed water samples were analysed regularly. The experiments were executed at room temperature with a transmembrane pressure (TMP) of 4.5–5.5 bar, and flux of $50–60\ L{\cdot}(m^2{\cdot}h)^{-1}$, which is a regular to high flux for these type of membranes [18,32–34]. The cross-flow velocity was $1.0–1.2\ m{\cdot}s^{-1}$ resulting in a turbulent flow with a Reynold number of 4200, as recommended by the suppliers. The following equation (Eq. (1)) was used to calculate the temperature-corrected permeability:

$$L_{20\text{Â°C}} = \frac{J \cdot e^{-0.0239\cdot(T-20)}}{\Delta P} \tag{1}$$

where, $L_{20^{\circ}C}$ is the temperature-corrected permeability at 20 °C ($L{\cdot}(m^2{\cdot}h{\cdot}bar)^{-1}$), T is temperature of water (°C), J is membrane flux ($L{\cdot}(m^2{\cdot}h)^{-1}$), and ΔP is transmembrane pressure (bar). All permeability values were temperature-corrected to 20 °C [35].

2.2.1. Hydraulic permeability

A demineralised water filtration test was performed before each filtration experiment to determine the initial hydraulic permeability. These hydraulic permeability tests were executed under similar conditions as the filtration tests with a duration of 1 h.

2.2.2. Filtration with salt solution

Phosphate retention tests were performed according to the filtration conditions mentioned earlier. The feed solution contained 1 mM NaCl salt, which served as a background to reduce the effect of pH adjustment on the salinity, and it was comparable with the concentration in municipal sewage [7,36]. Multivalent anions and cations were added to the salt solution to test their effect in a concentration of 0.3 mM H_2NaPO_4, and/or 0.3 mM $MgCl_2$ (Table 1). These concentrations were chosen in the range of municipal sewage.

The retention tests were executed in the pH range 5 to 9, while the pH was adjusted using NaOH or HCl. In order to maintain a pH of 9 in the feed tank, a nitrogen blanket was created over the feed tank using nitrogen gas. Then, feed, concentrate and permeate samples were taken for analysing the phosphate retention. These samples were taken 60 min after the pH adjustment to ensure stabilisation of the system.

2.2.3. Filtration with model sewage

Fouling tests were performed using sodium alginate as model compound for sewage [37,38]. The feed water composition consisted of $0.8\ g{\cdot}L^{-1}$ sodium alginate (Sigma-Aldrich), 1 mM NaCl (Sigma-Aldrich) as background salt concentration, 1 mM $NaHCO_3$ (Sigma-Aldrich) as buffer, and 3 mM $CaCl_2$ (Sigma-Aldrich) adjusted to pH of 7. Sodium alginate is known to form a gel in the presence of calcium ions and to aggregate according to the "egg-box" model which promotes cake layer development during filtration [38–41]. With the concentrated model sewage a pre-sieved municipal sewage experiment of 5 days could be simulated in two hours with the same membrane type [7].

As preparation for the streaming potential experiments of membranes with a fouling layer, the disc membranes were filtered with model sewage. During filtration the TMP was kept constant at 4 bar at a turbulent flow with a cross-flow velocity of 6.0–7.0 $m \cdot s^{-1}$, as recommended by the supplier. Followed by a forward flush to maintain merely the irreversible fouling on the membrane.

2.2.4. Retention tests

During filtration samples were taken to monitor the retention of the ions. The retention of ions R_i was calculated using Eq. (2).

$$R_i = \left(1 - \frac{c_{i,p}}{c_{i,c}}\right) \cdot 100\% \tag{2}$$

where $c_{p,i}$ is the ion concentration in the permeate and $c_{i,c}$ the ion concentration in the concentrate water.

2.2.5. Chemical cleaning

After each experiment using model sewage, the membranes were chemically cleaned with sodium hypochlorite to remove all fouling. Sodium hypochlorite is known as the most effective cleaning agent for (organically) fouled ceramic membranes [7,19,42,43]. The chemical cleaning was carried out by soaking the membranes in a 0.1% sodium hypochlorite solution for 1 h. The permeability recovery was > 97% after chemical cleaning.

After each experiment using a salt solution, the membranes were chemically cleaned by soaking the membranes in a 0.01 M sodium hydroxide solution for 15 min. Followed by a demin water filtration of two hours under similar conditions as the filtration test to flush the membranes. The permeability recovery was > 97%. After four experiments using salt solution, a chemical cleaning using sodium hypochlorite was carried out, as described above.

2.3. Analytical methods

2.3.1. Ion chromatography

The ion composition of the concentrate and permeate water were analysed using a ProfIC 15–AnCat ion chromatograph (Metrohm 881 anion (suppressed) and 883 cation system, Metrohm, Switzerland). Prior to these analyses the aqueous samples were filtered through 0.45 µm filters (Whatman, Germany). An A Supp 150/4.0 anion column was used with 3.2 mM Na_2CO_3 and 1 mM $NaHCO_3$ eluent for anions. For the cations a C5 cation column with 3 mM HNO_3 eluent was used. The regeneration solution, used for the suppressor, was 50 mM H_2SO_4.

2.3.2. Streaming potential experiments

In order to determine the membrane surface charge, the zeta potential was calculated by measuring the streaming potential. Disc membranes were used for this experiment because the streaming potential can only be determined on a flat membrane surface. The streaming potential of the ceramic NF membrane was determined using a SurPASS electro kinetic analyser (Anton Paar GmbH, Austria). The zeta potential was determined with the Helmholtz-Smoluchowski equation. Several solutions with various ionic compositions were analysed, all with an total ionic strength of 10 mM; 0.3 mM of the different ions – NaH_2PO_4, $MgCl_2$ and $NaSO_4$ – were present in a NaCl salt solution. KCl solution is most commonly used for streaming potential measurements. Puhlfürß et al. [18] found that using NaCl solution for streaming potential measurements is comparable with using KCl solution, when using similar ceramic NF membranes. Since NaCl is present in municipal sewage this was used during the measurements.

2.3.3. MWCO analysis

The MWCO of ceramic NF membranes was regularly measured to monitor the quality of the membranes, using the method described by Tam & Tremblay (1991), also used in other studies [44–48].

First, a mixture of five different polyethylene glycol (PEG) molecules (200, 300, 400, 600, and 1000 Da) (Sigma-Aldrich), each in a concentration of 6 $mg \cdot L^{-1}$, was filtered using a clean ceramic NF membrane. The same settings were used during filtration as described for the hydraulic permeability.

Then, the feed and permeate samples were analysed using HPLC (Shimadzu) equipped with size exclusion chromatography columns (SEC, 5 µm 30 Å PSS SUPREMA) and a RID-20A refractive index detector. The carrier liquid in the HPLC was ultrapure water at a flow rate of 1 $mL \cdot min^{-1}$. From the HPLC analyses, the molecular weight distribution curves of the dissolved PEG molecules in the feed and permeate were derived. These were converted into retention curves by calculating the rejection percentage of a PEG with a certain molecular weight (R_i) using Eq. (3):

$$R_i\,(\%) = \left(\frac{c_{i,feed} - c_{i,permeate}}{c_{i,feed}}\right) \cdot 100\% \tag{3}$$

where $c_{i,\ feed}$ is the PEG concentration in the feed samples and $c_{i,\ permeate}$ in the permeate samples.

Afterwards, the experimental retention curves were described by a log-normal model as function of molecular weight (*MW*) and MWCO using Eq. (4) [45,46,49]. Eq. (4) was used to model retention curve to be able to calculate the MWCO.

$$\sigma(MW_s) = \int_0^{MW_s} \frac{1}{s_{MW}\sqrt{2\pi}} \cdot \frac{1}{MW} \cdot exp\left[-\frac{(\ln(MW) - \ln(MWCO) + 0.56 \cdot s_{MW})^2}{2 \cdot s_{MW}^2}\right] \cdot dMW \tag{4}$$

where $\sigma(MW_s)$ is the reflection coefficient for a PEG with a molecular weight MW_s and s_{MW} is the standard deviation of the molecular weight distribution.

In this method, the separation of the PEG molecules is assumed to be only based on size exclusion with negligible solute diffusion. Therefore, the molecular size of the PEG solutes (d_s in nm) is correlated to their molecular weight (*MW* in Da) as shown in Eq. (5) [45,49].

$$d_s = 0.065 \cdot MW^{0.438} \tag{5}$$

Finally, the MWCO was estimated at 90% of the retention curve [35,46].

3. Results & discussion

3.1. Determination of MWCO

Previous research has shown that the quality of these membranes can vary within one batch [33]. Therefore, the quality of the three ceramic NF membranes, used in this study, was determined before and after each experiment by calculating the MWCO. The initial MWCO was measured to be 500, 503, and 549 Da, respectively, and remained stable throughout the experiments. The streaming potential experiments were performed with two disc membranes with a measured MWCO of 495 and 538 Da.

3.2. Influence of pH on the retention of phosphate by clean membranes

The phosphate retention during ceramic NF with clean membranes was measured in a salt solution at pH varying from 5 to 9. The phosphate retention increased with the pH from 76% to 99%, respectively (Fig. 1). The phosphate was not rejected due to size exclusion, since the pore size of the ceramic NF membranes is around 0.9 nm (according to the supplier) and the hydraulic radii of phosphate, in the forms $H_2PO_4{}^{-}$ and $HPO_4{}^{2-}$, are 0.302 and 0.327 nm, respectively [8,50]. Thus, electrostatic repulsion, probably, played a decisive role in retention.

With an increasing pH, from 5 to 9, phosphate shifts from a monovalent ($H_2PO_4{}^{-}$) to a divalent ($HPO_4{}^{2-}$) form. The divalent form has a lower diffusion coefficient ($7.34 \cdot 10^{10}$ $m \cdot s^{-2}$) than the monovalent

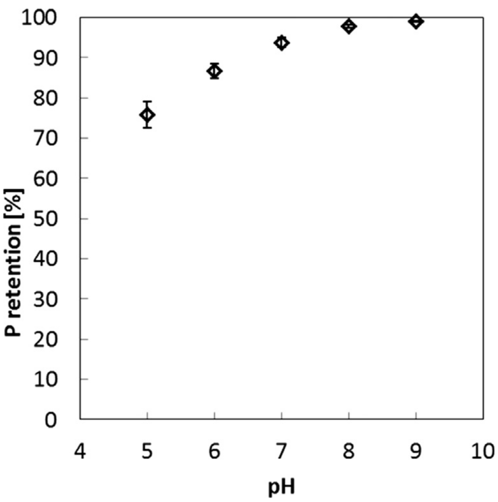

Fig. 1. Retention curve of phosphate for a pH range of 5–9 during ceramic NF in 0.01 M salt solution.

form ($8.46{\cdot}10^{10}\ m{\cdot}s^{-2}$)[51], which possibly enhanced the retention at higher pH.

To confirm the role of electrostatic repulsion, the membrane surface charge was determined by measuring the streaming potential from which the zeta potential can be calculated (Fig. 2). The results show that the zeta potential of the membranes was negative, −8 to −22 mV for pH 4 to 9, respectively. Upon addition of phosphate to the solution the negative membrane charge increased to −28 to −39 mV, respectively, in the same pH range (Fig. 2). This probably caused the increase in phosphate retention at high pH (Fig. 1). Apparently, phosphate adsorbed on the membrane surface, resulting in a more negatively charged membrane which is referred to as specific adsorption. This was also observed by Shang et al. [20,52] when using ceramic UF membranes of similar material.

Puhlfürß et al. [18] also determined the zeta potential of similar ceramic NF membranes, but in a broader pH range, from 2.5 to 10.5. They found the isoelectric point to be at pH 3.3. At pH 4 the zeta potential was comparable to the results in Fig. 2, albeit with increasing pH the zeta potential decreased faster, to −33 mV instead of −22 mV at pH 9. However, Puhlfürß et al. [18] used a lower concentration of NaCl solution, which probably caused a higher negative membrane charge. This effect on the membrane charge was also observed by Afonso et al. and Deon et al. [23,24].

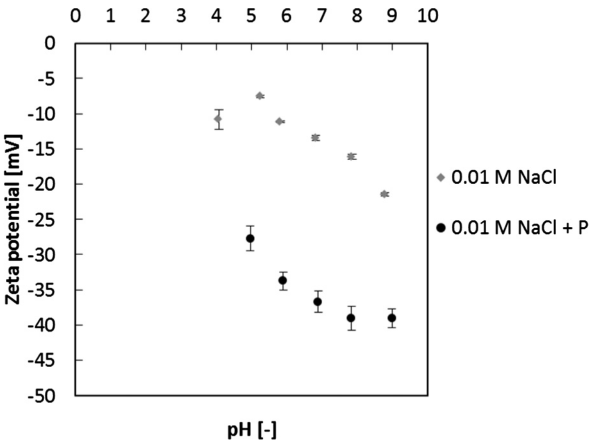

Fig. 2. Zeta potential of ceramic NF membrane at a pH range of 4–9 using a solution of 0.01 M NaCl (diamonds) or 0.01 M NaCl with phosphate (dots).

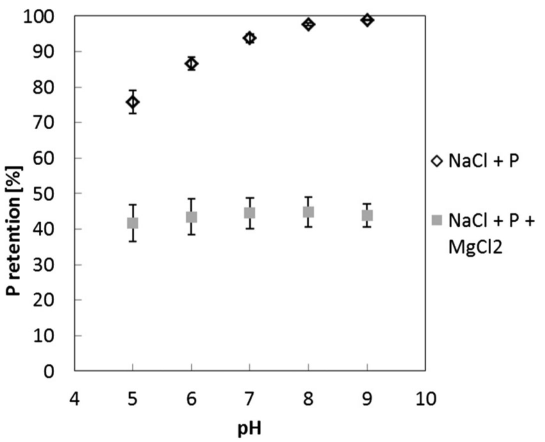

Fig. 3. Retention curve of phosphate for a pH range of 5–9 during ceramic NF. The effect of $MgCl_2$ on phosphate retention was determined.

3.3. Influence of multivalent counter ions on the retention of phosphate by clean membranes

Co-existent ions could have an (negative) effect on the phosphate retention, in particular, multivalent cations that are present in sewage. Therefore, first, the phosphate retention was analysed in the presence of $MgCl_2$ (0.3 mM), added to the salt solution that included phosphate. $MgCl_2$ addition caused a drop in phosphate retention: 42% at pH 5, ranging to 44% for pH 9 (Fig. 3). Moreover, the zeta potential showed a lower negative charge in the presence of $MgCl_2$, from −12 to −27 mV in the pH range from 4 to 9, respectively, compared to the membrane charge measured in the solution with only NaCl and phosphate (Fig. 4).

Furthermore, Chevereau et al. [22] observed that magnesium ions have the ability to adsorb to negatively charged ceramic UF membranes. When this happens the membrane charge can even switch from negative to positive due to the charge of the magnesium ion. Another phenomenon described in literature is that divalent ions, such as magnesium, can suppress the diffuse double layer on the membrane surfaces [25,31,53]. The distinction between the two described phenomena could not be made with the zeta potential calculations because streaming potential is measured in the diffuse double layer, so both adsorption and diffuse double layer suppression were determined.

3.4. Influence of fouling layer on the retention of phosphate

Subsequently, model sewage was used to examine the effect of a fouling layer on the phosphate retention. Phosphate was added during

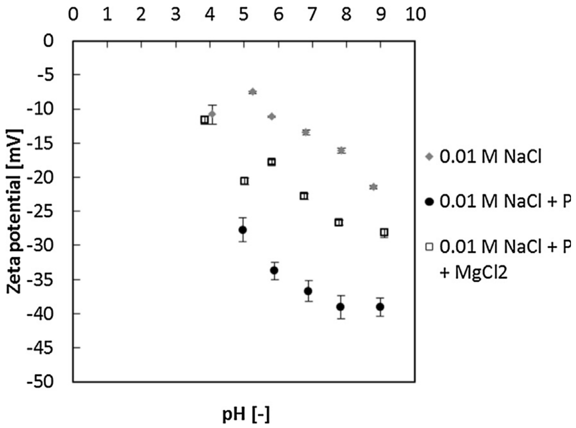

Fig. 4. Zeta potential of ceramic NF membrane at a pH range of 4–9 using a solution NaCl (squares), NaCl with phosphate (dots), and NaCl with phosphate and $MgCl_2$ (squares) with a total ionic strength of 0.01 M.

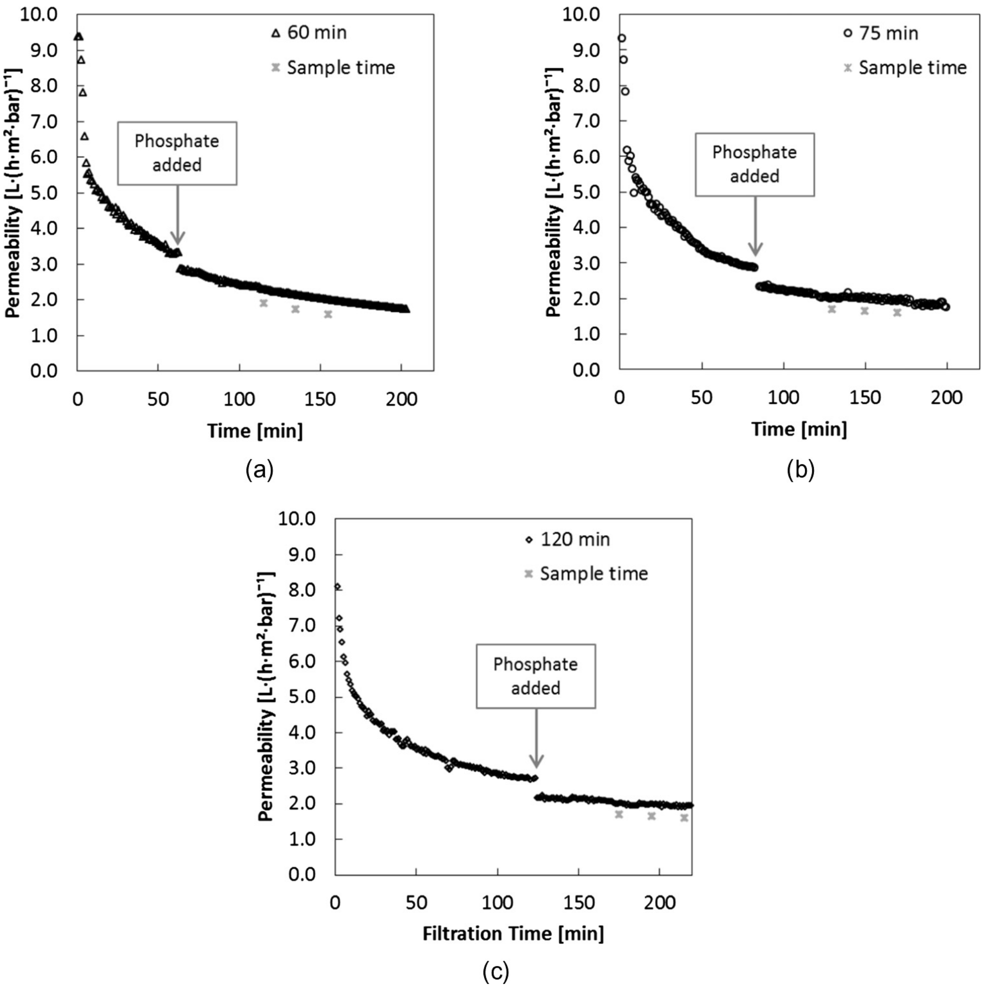

Fig. 5. a–c: Fouling experiments of ceramic NF using model sewage at pH of 7. (a–c) Permeability in time. Phosphate was added to the feed solution after 60, 75, and 120 min filtration. Three samples were taken (grey crosses).

filtration of model sewage to analyse the effect on the permeability and the phosphate retention. In order to also examine the influence of the thickness of the fouling layer, phosphate was added after 60, 75, and 120 min of filtration. Then, when the system stabilised, the phosphate retention was determined (see grey crosses in Fig. 5a–c).

An additional, clear, drop in permeability was visible due to the addition of phosphate (Fig. 5a–c). This might have been caused by the cake-enhanced concentration polarisation [17,27,31]. Another explanation of the drop could be the compaction of the cake layer in the presence of phosphate which made the cake layer less penetrable, resulting in a lower permeability [54]. The permeability drop was 0.85 L·(m^2·h·bar)$^{-1}$ after 60 min of filtration, 0.82 L·(m^2·h·bar)$^{-1}$ after 75 min of filtration, and 0.85 L·(m^2·h·bar)$^{-1}$ after 120 min of filtration, respectively.

The phosphate retention stabilised at 43–44% in the presence of a cake layer. Thus, the fouling layer on the membrane surface had a large impact on the phosphate retention (Fig. 6), when compared to clean membranes without fouling layer which had a phosphate retention of 94% (Fig. 1). This could be explained by the occurrence of cake-enhanced concentration polarisation: when the concentration of phosphate is higher on the membrane surface due to cake-enhanced concentration polarisation, the concentration of phosphate was higher in the permeate which caused a lower phosphate retention.

It should be noted that the flux was lower when the phosphate retention was measured in the presence of a cake layer than with a clean membrane. A known phenomena in membrane filtration is the dilution effect: at higher permeate flux, a higher retention of solvents is observed due to enhance convective transport [55]. In this case the reverse dilution effect could explain part of the lower phosphate retention measured in the presence of a cake layer, because the flux was about 5 times lower than without the presence of a cake layer. When assuming that the diffusion of phosphate is not changing due to the fouling layer, it can be calculated that the rejection of the pristine

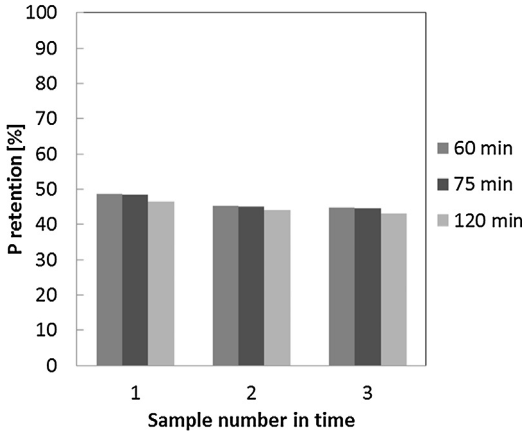

Fig. 6. Retention curve of phosphate during ceramic NF with model sewage. Phosphate was added after 60, 75, and 120 min of filtration (dark grey, black, and light grey, respectively). When the system stabilised three samples were taken (grey crosses in Fig. 5a–c).

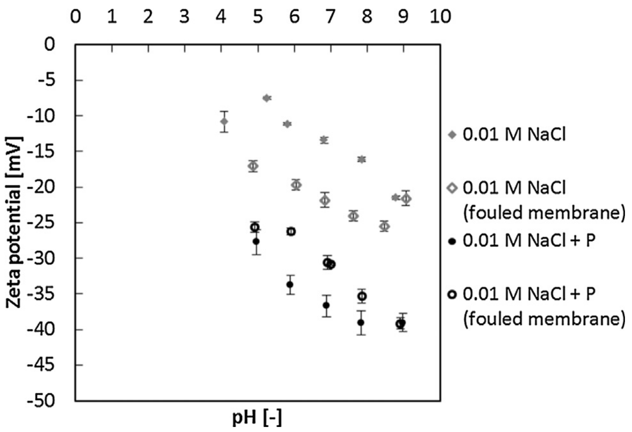

Fig. 7. Zeta potential of ceramic NF membrane at a pH range of 4–9 using a solution of 0.01 M NaCl (diamonds) and NaCl with phosphate (dots) for membranes with and without a fouling layer. The fouled membranes were prepared by filtering model sewage for over 2 h.

membrane of 94% (at pH 7) is decreasing to about 70% when the flux decreases 5 times (5 times higher permeate concentration). So, the lower flux cannot fully explain the measured decrease of the phosphate rejection.

The results of the zeta potential analysis of ceramic NF membranes with and without a fouling layer are presented in Fig. 7. When compared to the clean membranes in a NaCl solution, the membranes with fouling layer were more negatively charged. This can be explained by the negative charge of sodium alginate present in the model sewage [17,56]. However, when phosphate was present in the solution, the membranes without fouling layer were more negatively charged (−37 mV at pH 7) than in the presence of the fouling layer (−31 mV at pH 7) (Fig. 7). This could indicate that the fouling layer reduced the effect of the phosphate adsorption on the membrane layer which lead to a lower phosphate retention. Thus, three phenomena caused the reduction of the phosphate retention: (i) cake-enhanced concentration polarisation, (ii) the reverse dilution effect, and (iii) the lower zeta potential of the membranes.

4. Conclusions

In this paper the phosphate retention during ceramic NF was reported for phosphate reclamation purposes from municipal sewage. The phosphate retention during ceramic NF in a (monovalent) salt solution was 76 to 99% for a pH from 5 to 9, respectively, probably due to electrostatic repulsion. Specific adsorption of phosphate onto the membrane surface increased the membrane charge and thus the electrostatic repulsion. However, this effect was negatively influenced by multivalent counter ions such as magnesium, resulting in a drop in phosphate retention to only 42 to 44% for a change in pH from 5 to 9, respectively. The phosphate retention was lower due to a lower zeta potential which was caused either by adsorption of magnesium ions on the membrane surface and/or suppression of the diffuse double layer due to presence of magnesium ions.

The fouling on ceramic NF membranes also reduced the phosphate retention (43–44%). Even though the model foulant sodium alginate is negatively charged, the zeta potential on the membrane surface decreased in the presence of the fouling layer compared to a clean membrane. Moreover, occurrence of cake-enhanced concentration polarisation and the reverse dilution effect also contributed to the reduced phosphate retention in the presence of a cake layer.

Acknowledgements

The research presented in this paper was supported by the STW, the Netherlands grant (Project Number 13346) and is part of the Rotterdam Innovative Nutrients Energy and Water (RINEW) project led by Evides Industriewater. The authors would like to acknowledge Antoine Kemperman, Bob Siemerink, and Iske Achterhuis of University of Twente for the streaming potential measurements. Finally, thanks to Anna Ciafalo and Herman Kramer for their contribution to this research.

References

[1] J.-O. Drangert, Phosphorus–a limited resource that could be made limitless, Procedia Eng. 46 (2012) 228–233, https://doi.org/10.1016/j.proeng.2012.09.469.
[2] D. Cordell, J.-O. Drangert, S. White, The story of phosphorus: global food security and food for thought, Glob. Environ. Change 19 (2009) 292–305, https://doi.org/10.1016/j.gloenvcha.2008.10.009.
[3] P.L. McCarty, J. Bae, J. Kim, Domestic wastewater treatment as a net energy producer–can this be achieved? Environ. Sci. Technol. 45 (2011) 7100–7106, https://doi.org/10.1021/es2014264.
[4] R.C. Wielemaker, J. Weijma, G. Zeeman, Resources, conservation and recycling harvest to harvest : recovering nutrients with new sanitation systems for reuse in urban agriculture, Resour. Conserv. Recycl. 128 (2018) 426–437, https://doi.org/10.1016/j.resconrec.2016.09.015.
[5] R. Butler, T. Maccormick, Opportunities for decentralized treatment, sewer mining and effluent re-use, Desalination 106 (1996) 273–283.
[6] M. Xie, L.D. Nghiem, W.E. Price, M. Elimelech, A forward osmosis-membrane distillation hybrid process for direct sewer mining: system performance and limitations, Environ. Sci. Technol. 47 (2013) 13486–13493, https://doi.org/10.1021/es404056e.
[7] F.C. Kramer, R. Shang, S.G.J. Heijman, S.M. Scherrenberg, J.B. van Lier, L.C. Rietveld, Direct water reclamation from sewage using ceramic tight ultra- and nanofiltration, Sep. Purif. Technol. (2015) 1–21, https://doi.org/10.1111/j.1747-6593.2011.00271.x.Olsson.
[8] B. Tansel, J. Sager, T. Rector, J. Garland, R.F. Strayer, L. Levine, M. Roberts, M. Hummerick, J. Bauer, Significance of hydrated radius and hydration shells on ionic permeability during nanofiltration in dead end and cross flow modes, Sep. Purif. Technol. 51 (2006) 40–47, https://doi.org/10.1016/j.seppur.2005.12.020.
[9] N.S. Kotrappanavar, A.A. Hussain, M.E.E. Abashar, I.S. Al-Mutaz, T.M. Aminabhavi, M.N. Nadagouda, Prediction of physical properties of nanofiltration membranes for neutral and charged solutes, Desalination 280 (2011) 174–182, https://doi.org/10.1016/j.desal.2011.07.007.
[10] J. Schaep, C. Vandecasteele, Evaluating the charge of nanofiltration membranes, J. Membr. Sci. 188 (2001) 129–136, https://doi.org/10.1016/S0376-7388(01)00368-4.
[11] M. Nyström, L. Kaipia, S. Luque, Fouling and retention of nanofiltration membranes, J. Membr. Sci. 98 (1995) 249–262, https://doi.org/10.1016/0376-7388(94)00196-6.
[12] J.D. Doyle, S.A. Parsons, Struvite formation, control and recovery, Water Res. 36 (2002) 3925–3940.
[13] L. Shu, P. Schneider, V. Jegatheesan, J. Johnson, An economic evaluation of phosphorus recovery as struvite from digester supernatant, Bioresour. Technol. 97 (2006) 2211–2216, https://doi.org/10.1016/j.biortech.2005.11.005.
[14] W. Verstraete, P. Van de Caveye, V. Diamantis, Maximum use of resources present in domestic "used water", Bioresour. Technol. 100 (2009) 5537–5545, https://doi.org/10.1016/j.biortech.2009.05.047.
[15] E.V. Münch, K. Barr, Controlled struvite crystallisation for removing phosphorus from anaerobic digester sidestreams, Water Res. 35 (2001) 151–159 http://www.ncbi.nlm.nih.gov/pubmed/11257869.
[16] S.J. Lee, M. Dilaver, P.K. Park, J.H. Kim, Comparative analysis of fouling characteristics of ceramic and polymeric microfiltration membranes using filtration models, J. Membr. Sci. 432 (2013) 97–105, https://doi.org/10.1016/j.memsci.2013.01.013.
[17] Y. Zhao, X. Wang, H. Yang, Y.F. Xie, Effects of organic fouling and cleaning on the retention of pharmaceutically active compounds by ceramic nanofiltration membranes, J. Membr. Sci. 563 (2018) 734–742, https://doi.org/10.1016/j.memsci.2018.06.047.
[18] P. Puhlfürß, A. Voigt, R. Weber, M. Morbé, Microporous TiO2 membranes with a cut off < 500 Da, J. Membr. Sci. 174 (2000) 123–133, https://doi.org/10.1016/S0376-7388(00)00380-X.
[19] Z. Cui, W. Peng, Y. Fan, W. Xing, N. Xu, Effect of cross-flow velocity on the critical flux of ceramic membrane filtration as a pre-treatment for seawater desalination, Chin. J. Chem. Eng. 21 (2013) 341–347, https://doi.org/10.1016/S1004-9541(13)60470-X.
[20] R. Shang, A.R.D. Verliefde, J. Hu, Z. Zeng, J. Lu, A.J.B. Kemperman, H. Deng, K. Nijmeijer, S.G.J. Heijman, L.C. Rietveld, Tight ceramic UF membrane as RO pretreatment: the role of electrostatic interactions on phosphate rejection, Water Res. 48 (2014) 498–507, https://doi.org/10.1016/j.watres.2013.10.008.
[21] T. Tsuru, D. Hironaka, T. Yoshioka, M. Asaeda, Effect of divalent cations on permeate volume flux through porous titania membranes, Desalination 147 (2002) 213–216, https://doi.org/10.1016/S0011-9164(02)00536-2.
[22] E. Chevereau, N. Zouaoui, L. Limousy, P. Dutournié, S. Déon, P. Bourseau, Surface properties of ceramic ultrafiltration TiO2 membranes: effects of surface equilibriums on salt retention, Desalination 255 (2010) 1–8, https://doi.org/10.1016/j.desal.2009.12.007.

[23] M.D. Afonso, G. Hagmeyer, R. Gimbel, Streaming potential measurements to assess the variation of nanofiltration membranes surface charge with the concentration of salt solutions, Sep. Purif. Technol. 22–23 (2001) 529–541, https://doi.org/10.1016/S1383-5866(00)00135-0.

[24] S. Déon, A. Escoda, P. Fievet, A transport model considering charge adsorption inside pores to describe salts rejection by nanofiltration membranes, Chem. Eng. Sci. 66 (2011) 2823–2832, https://doi.org/10.1016/j.ces.2011.03.043.

[25] R.J. Hunter, Zeta potential in colloid science : principles and applications, 1981.

[26] P. Dutournié, L. Limousy, J. Anquetil, S. Déon, Modification of the selectivity properties of tubular ceramic membranes after alkaline treatment, Membranes (Basel) 7 (2017) 65, https://doi.org/10.3390/membranes7040065.

[27] E.M.V. Hoek, M. Elimelech, Cake-enhanced concentration polarization: a new fouling mechanism for salt-rejecting membranes, Environ. Sci. Technol. 37 (2003) 5581–5588, https://doi.org/10.1021/es0262636.

[28] A.R.D. Verliefde, E.R. Cornelissen, S.G.J. Heijman, J.Q.J.C. Verberk, G.L. Amy, B. Van Der Bruggen, J.C. Van Dijk, The role of electrostatic interactions on the rejection of organic solutes in aqueous solutions with nanofiltration, J. Membr. Sci. 322 (2008) 52–66, https://doi.org/10.1016/j.memsci.2008.05.022.

[29] N. García-Martín, V. Silva, F.J. Carmona, L. Palacio, A. Hernández, P. Prádanos, Pore size analysis from retention of neutral solutes through nanofiltration membranes. The contribution of concentration–polarization, Desalination 344 (2014) 1–11, https://doi.org/10.1016/j.desal.2014.02.038.

[30] J.E. Kilduff, S. Mattaraj, G. Belfort, Flux decline during nanofiltration of naturally-occurring dissolved organic matter : effects of osmotic pressure, membrane permeability, and cake formation, J. Membr. Sci. 239 (2004) 39–53, https://doi.org/10.1016/j.memsci.2003.12.030.

[31] J. Wang, D.S. Dlamini, A.K. Mishra, M.T.M. Pendergast, M.C.Y. Wong, B.B. Mamba, V. Freger, A.R.D. Verliefde, E.M.V. Hoek, A critical review of transport through osmotic membranes, J. Membr. Sci. 454 (2014) 516–537, https://doi.org/10.1016/j.memsci.2013.12.034.

[32] I. Voigt, H. Richter, M. Stahn, M. Weyd, P. Puhlfürß, V. Prehn, C. Günther, Scale-up of ceramic nanofiltration membranes to meet large scale applications, Sep. Purif. Technol. 215 (2019) 329–334, https://doi.org/10.1016/j.seppur.2019.01.023.

[33] F.C. Kramer, R. Shang, S.M. Scherrenberg, L.C. Rietveld, S.J.G. Heijman, Quantifying defects in ceramic tight ultra- and nanofiltration membranes and investigating their robustness, Sep. Purif. Technol. 219 (2019) 159–168, https://doi.org/10.1016/j.seppur.2019.03.019.

[34] T. Fujioka, S.J. Khan, J.A. McDonald, L.D. Nghiem, Nanofiltration of trace organic chemicals: a comparison between ceramic and polymeric membranes, Sep. Purif. Technol. 136 (2014) 258–264, https://doi.org/10.1016/j.seppur.2014.08.039.

[35] M. Mulder, Basic principles of membrane technology, Zeitschrift Für Phys Chemie (1996) 564, https://doi.org/10.1524/zpch.1998.203.Part_1_2.263.

[36] H. Ozgun, Y. Tao, M.E. Ersahin, Z. Zhou, J.B. Gimenez, H. Spanjers, J.B. van Lier, Impact of temperature on feed-flow characteristics and filtration performance of an upflow anaerobic sludge blanket coupled ultrafiltration membrane treating municipal wastewater, Water Res. (2015), https://doi.org/10.1016/j.watres.2015.06.035.

[37] Y. Ye, P. Le Clech, V. Chen, A.G. Fane, B. Jefferson, Fouling mechanisms of alginate solutions as model extracellular polymeric substances, Desalination 175 (2005) 7–20, https://doi.org/10.1016/j.desal.2004.09.019.

[38] K. Katsoufidou, S.G. Yiantsios, A.J. Karabelas, Experimental study of ultrafiltration membrane fouling by sodium alginate and flux recovery by backwashing, J. Memb. Sci. 300 (2007) 137–146, https://doi.org/10.1016/j.memsci.2007.05.017.

[39] P. van den Brink, A. Zwijnenburg, G. Smith, H. Temmink, M. van Loosdrecht, Effect of free calcium concentration and ionic strength on alginate fouling in cross-flow membrane filtration, J. Membr. Sci. 345 (2009) 207–216, https://doi.org/10.1016/j.memsci.2009.08.046.

[40] F. Zhao, K. Xu, H. Ren, L. Ding, J. Geng, Y. Zhang, Combined effects of organic matter and calcium on biofouling of nanofiltration membranes, J. Membr. Sci. 486 (2015) 177–188, https://doi.org/10.1016/j.memsci.2015.03.032.

[41] L.U. Alazmi, Radhi, The effect of wastewater components on the fouling of ceramic membranes, 2010.

[42] M. Lee, Z. Wu, K. Li, 2 – Advances in ceramic membranes for water treatment, 2015. doi:https://doi.org/10.1016/B978-1-78242-121-4.00002-2.

[43] M. Zebić Avdičević, K. Košutić, S. Dobrović, Effect of operating conditions on the performances of multichannel ceramic UF membranes for textile mercerization wastewater treatment, Environ. Technol. (United Kingdom) 38 (2017) 65–77, https://doi.org/10.1080/09593330.2016.1186225.

[44] C.M. Tam, A.Y. Tremblay, Membrane pore characterization-comparison between single and multicomponent solute probe techniques, J. Membr. Sci. 57 (1991) 271–287, https://doi.org/10.1016/S0376-7388(00)80683-3.

[45] J. Shirley, S. Mandale, V. Kochkodan, Influence of solute concentration and dipole moment on the retention of uncharged molecules with nanofiltration, Desalination 344 (2014) 116–122, https://doi.org/10.1016/j.desal.2014.03.024.

[46] B. Van Der Bruggen, C. Vandecasteele, Modelling of the retention of uncharged molecules with nanofiltration, Water Res. 36 (2002) 1360–1368, https://doi.org/10.1016/S0043-1354(01)00318-9.

[47] S. Blumenschein, A. Böcking, U. Kätzel, S. Postel, M. Wessling, Rejection modeling of ceramic membranes in organic solvent nanofiltration, J. Membr. Sci. 510 (2016) 191–200, https://doi.org/10.1016/j.memsci.2016.02.042.

[48] C. Causseranda, P. Aim, C. Vilani, T. Zambellib, Study of the effects of defects in ultrafiltration membranes on the water flux and the molecular weight cut-off, Desalination 149 (2002) 485–491.

[49] R. Shang, A. Goulas, C.Y. Tang, X. de Frias Serra, L.C. Rietveld, S.G.J. Heijman, Atmospheric pressure atomic layer deposition for tight ceramic nanofiltration membranes: synthesis and application in water purification, J. Membr. Sci. 528 (2017) 163–170, https://doi.org/10.1016/j.memsci.2017.01.023.

[50] M.Y. Kiriukhin, K.D. Collins, Dynamic hydration numbers for biologically important ions, Biophys. Chem. 99 (2002) 155–168.

[51] D. Krom, R.A. Berner, The diffusion coefficients of sulfate, ammonium, phosphate ions in anoxic marine sediments, Limnol. Oceanogr. 25 (1980) 327–337.

[52] R. Shang, A.R.D. Verliefde, J. Hu, S.G.J. Heijman, L.C. Rietveld, The impact of EfOM, NOM and cations on phosphate rejection by tight ceramic ultrafiltration, Sep. Purif. Technol. 132 (2014) 289–294, https://doi.org/10.1016/j.seppur.2014.05.024.

[53] T. Tsuru, M. Narita, R. Shinagawa, T. Yoshioka, Nanoporous titania membranes for permeation and filtration of organic solutions, DES 233 (2008) 1–9, https://doi.org/10.1016/j.desal.2007.09.021.

[54] C. Visvanathan, B.D. Marsono, B. Basu, Removal of THMP by nanofiltration: effects of interference parameters, Water Res. 32 (1998) 3527–3538, https://doi.org/10.1016/S0043-1354(98)00151-1.

[55] J. Luo, Y. Wan, Effects of pH and salt on nanfiltration — a critical review, J. Membr. Sci. 438 (2013) 18–28, https://doi.org/10.1016/j.memsci.2013.03.029.

[56] A. Simon, W.E. Price, L.D. Nghiem, Changes in surface properties and separation efficiency of a nanofiltration membrane after repeated fouling and chemical cleaning cycles, Sep. Purif. Technol. 113 (2013) 42–50, https://doi.org/10.1016/j.seppur.2013.04.011.